Explosion characteristics of intense femtosecond-laser-driven water droplets

M. Schnürer,[1] D. Hilscher,[2] U. Jahnke,[2] S. Ter-Avetisyan,[1] S. Busch,[1] M. Kalachnikov,[1] H. Stiel,[1] P. V. Nickles,[1] and W. Sandner[1]

[1]*Max-Born-Institut, Max-Born-Strasse 2a, D-12489 Berlin, Germany*

[2]*Hahn-Meitner-Institut, Glienickerstrasse 100, D-14109 Berlin, Germany*

(Received 30 March 2004; revised manuscript received 15 July 2004; published 5 November 2004)

An efficient acceleration of energetic ions is observed when small heavy-water droplets of $\sim 20\ \mu$m diameter are exposed to ultrafast (~ 40 fs) Ti:sapphire laser pulses of up to 10^{19} W/cm^2 intensity. Quantitative measurements of deuteron and neutron spectra were done, allowing one to analyze the outward and inward directed deuteron acceleration from the droplet. Neutron spectroscopy based on the D(d,n) fusion reaction was accomplished in four different spatial directions. The energy shifts of those fusion neutrons produced inside the exploding droplet reflect a remaining deuteron acceleration inside the irradiated droplet along the axis of the incident laser beam. The overall neutron yield of the microdroplets is relatively small as a result of the dominant outward directed acceleration of the deuterons with 1200 neutrons/shot. Relying on the "explosion-like" acceleration of such spherical droplet targets we have developed a spray target consisting of heavy-water microspheres with diameters of 150 nm. Both the high deuteron energies of up to 1 MeV resulting from the irradiation intensity of $\sim 10^{19}$ W/cm^2 as well as the collisions between the deuterons and the surrounding spray delivered about one order of magnitude more neutrons than the single-droplet system. The $\sim 6\times 10^3$ neutrons per laser pulse from the spray can be attributed to an efficient deuteron release from a significantly smaller laser excited volume as from deuterium-cluster targets.

DOI: 10.1103/PhysRevE.70.056401 PACS number(s): 52.38.Kd, 52.70.Nc, 29.30.Hs, 25.60.Pj

I. INTRODUCTION

When intense laser pulses with an intensity I and a wavelength λ interact with solid matter at $I\lambda^2 > 10^{18}$ (W/cm^2)μm^2 several percent of the incident energy is converted into kinetic energy of ions with up to several MeV per nucleon [1,2]. In general this phenomenon occurs because the intense laser field expels the electrons faster than the heavier ions such that a charge displacement occurs and the resulting large static electric field accelerates the ions. Different facets of the underlying physical processes (e.g., the target normal sheath acceleration mechanism [3]) are now being intensely studied to get a better understanding of the energy transport from the laser light to charged particles at such high intensities. Furthermore, the laser-produced intense ion beams constitute a source for further applications [4–6]. While the ion emission outside the target can be measured directly, the ion dynamics inside a dense target is difficult to access. Under these circumstances fusion neutron spectroscopy has been shown to be a powerful tool because neutrons produced in fusion reactions penetrate dense matter almost undisturbed while their energies reflect the ion collision kinematics [7,8].

Additionally several investigations have been performed to study laser-driven deuterium fusion with compact subpicosecond short pulse laser systems in order to establish short pulse neutron sources [8–13]. The advantage of such a neutron source lies in a relatively low laser energy input of a few hundred millijoules up to some joules per pulse and a neutron pulse length which is mainly determined by the source size. Thus one can anticipate for 2.45 MeV D(d,n)-fusion neutrons a pulse duration of ~ 5 ps in the near vicinity of 100 μm extended source. Given sufficient flux such a neutron pulse can be used to expose a piece of solid matter where—due to the heavy neutron impact—a change in its structure takes place. This structural change could be probed and temporally resolved with short x-ray pulses [14]. At present the insufficient neutron flux obtained hinders experiments of such type and motivates further investigation of laser-target concepts. The highest neutron yields ($\sim 10^7$ n in 4π sr) have been obtained from solid targets with laser pulses of 7 J energy [15]. In other work using lower energy laser pulses (0.3 J) and a solid target $\sim 10^4$ n in 4π sr have been reported [8,10].

Up to now clusterlike objects have been intensively studied in order to look for an efficient energy transfer from the laser radiation to the kinetic energy of ions. Due to their local high density in the isolated volume of a single cluster particle it is, in principle, possible to produce a high charge density, which is a prerequisite for the acceleration of the ions. Thus the interaction of high intensity laser radiation with large clusters (10^3 to 10^6 atoms per cluster) leads to an efficient transfer of laser energy to the kinetic energy of ionized atoms from the cluster [16]. But on the other hand these ions collide with an ambient medium of up to four orders of magnitude lower average density compared to a solid. This is partly compensated by setting a large interaction volume in the cluster cloud with an appropriate focused laser beam. Pure deuterium cluster targets [10] and deuterized clusters [11] showed values of about 10^4 neutrons per 4π sr and per incident laser pulse [12,14]. However, the measured deuteron kinetic energies from clusters are quite low and therefore not optimal for efficient neutron production. It was found that exploding CD_4 clusters exhibit only two times higher deuteron energies than D_2 clusters. Up to now deuteron energies of about 2.5 keV at a laser irradiation

of $\sim 10^{16}-10^{17}$ W/cm^2 [10] and 10–20 keV at $\sim 10^{19}-10^{20}$ W/cm^2 [12] have been measured from these cluster targets. Therefore it is interesting to look for target modifications that can overcome this disadvantage.

In this paper we describe experimental studies with deuterons accelerated by the interaction of high intensity laser pulses ($\sim 10^{19}$ W/cm^2) with heavy-water D_2O droplets. In general this interaction scenario is determined by the creation of huge electrical currents and the buildup of resulting acceleration potentials for the ions. It is much different from lower laser intensity interaction at longer pulses where an ablating plasma from the surface determines the ion kinematics. Whereas already several experiments at relativistic laser intensities have been regarding the interaction with flat surfaces and plane foil targets, only a little work has been realized with respect to small spherical targets. Due to their small and confined volume as well as their symmetry substantial differences from plane targets are likely, which has not been proven experimentally yet. As a significant extension to previous work [13] a multichannel spectrometer setup was realized in order to infer the ion kinematics from the experimental data. The analysis of the ion kinematics inside the dense droplet is based on the fusion reaction $d+\mathrm{D} \rightarrow {}^3\mathrm{He}+n+3.269$ MeV. The deuteron emission to the outside of the target has been directly measured. A detailed calibration of our spectrometer was important for the data analysis. In particular we tried to infer the yield of neutrons which is produced inside the target droplet. Taking these findings into account, a spray target [17,18] was developed in order to exploit and optimize the neutron production from laser-irradiated plasma spheres. The spray consists of microdroplets which are several orders of magnitude bigger than deuterium clusters used so far. This affects significantly the produced deuteron energy spectrum which gives rise to different properties if compared with cluster sources. The behavior of such a target system exposed to an intense laser field ($\sim 10^{19}$ W/cm^2) is studied and neutron emission from such a source is demonstrated for the first time to our knowledge.

After description of the experimental setup (Sec. II) we describe and discuss the findings with the single-droplet source in Secs. III–VII. A comparison to the results from the spray source will be done finally in Sec. VIII.

II. EXPERIMENTAL SETUP

The experiments have been carried out with ~40 fs laser pulses at 815 nm center wavelength from the MBI high-field Ti:sapphire laser [19]. For the present experiments, up to 600 mJ pulses in a beam of 70 mm in diameter are focused with an $f/2.5$ off axis parabolic mirror. Interaction intensities of $\sim 10^{19}$ W/cm^2 have been estimated from the energy content and pulse duration in a focal area with a diameter of ~ 6 μm. Heavy-water targets have been produced with a commercial and well-characterized [20] 1 MHz pulsed nozzle from Micro Jet Components (Sweden). A 10 Hz laser shot repetition was used in the experimental runs. The laser is focused 15 mm below the jet-nozzle outlet where the liquid jet is decomposed into a train of droplets. For the simulation calculations to be described below we assume a droplet diameter of ~ 20 μm and a droplet separation of 70 μm (center to center). This geometry is corroborated by measurements performed by Düsterer [21] with a similar nozzle. At a distance of about 4 cm from the nozzle the jet enters through an aperture a separately pumped water sink. The reaction chamber with a diameter of 70 cm and a wall thickness of 1 cm was pumped to a few times 10^{-5} mbar pressure when the water jet was on.

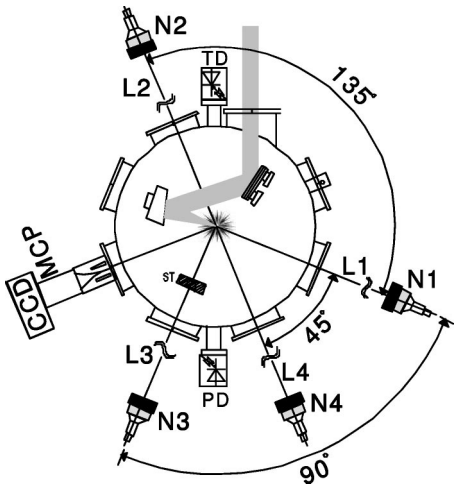

FIG. 1. Setup of the experiment with distances L1 (349 cm), L2 (326 cm), L3 (327 cm), and L4 (325 cm). PD, plasma diode; TD, diode used for timing.

In addition a pulsed water spray is used as a further target source. It exploits the expansion of superheated water through a nozzle into vacuum. Detailed characterization of the spray [17] gave a number density of droplets near the nozzle of 10^{11} droplets/cm^3 with a droplet diameter of 0.15 μm. The mean atomic density near the nozzle is greater than 10^{18} atoms/cm^3. The laser is focused at about 1 mm below the jet nozzle outlet where the spray has a radial extension of about 1 mm and a mean atomic density of about 10^{18} atoms/cm^3. In a Rayleigh range of $70\ \mu\mathrm{m} \times 2w_0 = 6$ μm about 200 microspheres are exposed to the focused laser radiation. The spray was injected only every 12 s in order to pump down the target chamber to a pressure of $\sim 10^{-4}$ mbar after each injection.

Secondary targets (STs) which have been exposed to the ions emitted from the laser irradiated primary droplet target (PDT) consisted of a 2 mg/cm^2 thick deuterated polystrol $(CD)_n$ foil on a 2 mm thick Al substrate. Either a disk of 4.5 cm outer diameter (and a 1.5 cm inner diameter hole) or a quadratic plate with an area of 9.5×9.5 cm^2 have been used at different angles and distances. These secondary targets have been employed to investigate the accuracy of the neutron detection efficiencies in the presence of a large gamma flash and to monitor the deuteron yield as will be explained below.

The arrangement of the detectors used in the experiment is schematically depicted in Fig. 1 and further notation concerning the target system is given in Fig. 2. A Thomson parabola spectrometer registered the ion emission at an observation angle of 135° (laser propagation direction corre-

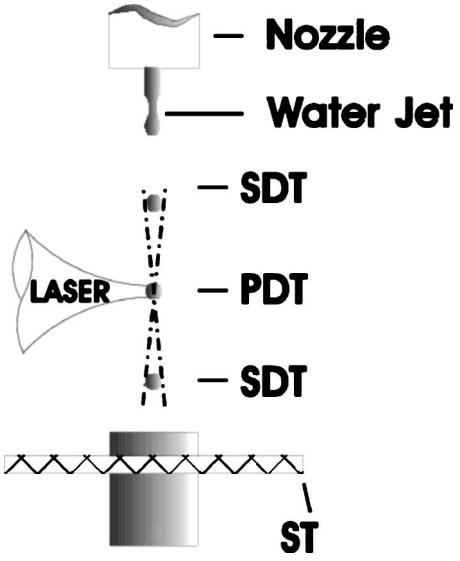

FIG. 2. Schematic of the droplet target system: The injected water jet decomposes into single droplets. SDT–secondary droplet target as a neighbor of the PDT–primary droplet target, ST- secondary target with a deuterized plastic coating (parameter cf. text)

sponds to 0°). The spectrometer entrance pinhole has a diameter of 200 μm in a lead plate of 1 mm thickness and is placed at a distance of 35 cm from the source. A microchannel plate (MCP) was used for ion detection. The pressure inside the spectrometer was typically at the order of $\sim 10^{-6}$ mbar. The phosphorus screen of the MCP was imaged with a cooled charge-coupled device (CCD) camera. The single-particle response of this detection system was evaluated with α-particle emission from an ^{241}Am source. Typically a magnetic field of about 0.27 T and electric fields of 2–6 kV/cm have been applied.

Four neutron detectors (N1–N4) were positioned at observation angles of 0°, 135°, 90°, and 45° relative to the laser beam at distances between 322 cm and 349 cm (cf. Fig. 1) viewing the target through 2 mm Al windows. The detectors consist of a liquid scintillator (NE213) with a diameter of 12.7 cm and a thickness of either 2.54 cm (N2, N3) or 5.08 cm (N1, N4) which is coupled to a 4 in. photomultiplier tube. Directly in front of each scintillator a 1 cm thick lead disk with a diameter of 15 cm and a 5 cm thick and 20 $\times 20$ cm^2 lead brick wall were positioned in order to reduce the amplitude of the prompt γ pulse. We intentionally avoided, however, sideward shielding which is particularly detrimental to the time resolution of neutrons [8]. On-line measured thresholds for the neutron detection were used to calculate the detector efficiencies. The tail of the prompt gamma flash might increase the thresholds. This introduces an systematic error in the absolute neutron intensity of about 30%.

The laser pulses were counted with an optical diode (TD in Fig. 1) which serves also as a trigger for the acquisition system incorporating the time of flight (TOF) neutron spectrometers. Another optical diode (PD) registered the plasma light emission attenuated through a colored-glass filter in a wavelength band between 350 nm and 600 nm. The signal of this diode was used as a marker of the laser droplet interaction. Since no precautions were taken to keep the droplet train in phase with the laser operation, as for instance was done in Ref. [20], the interaction probability is random and can be estimated easily from the droplet separation of about 70 μm between two droplets and a diameter of 20 μm at about 23%. This agrees quite well with the number of nonzero signals (above a certain threshold) of the plasma diode relative to the total number of laser shots, which varied between 0.3 and 0.4. This plasma diode (PD) was employed to normalize the measured neutron intensities on the number of laser shots which actually interacted with the droplets. All measured quantities are recorded as list-mode data with a multiparameter acquisition system [8]. For each laser shot a correlation analysis of all measured quantities is possible. The experimental runs comprised between 30 000 and 150 000 laser pulses.

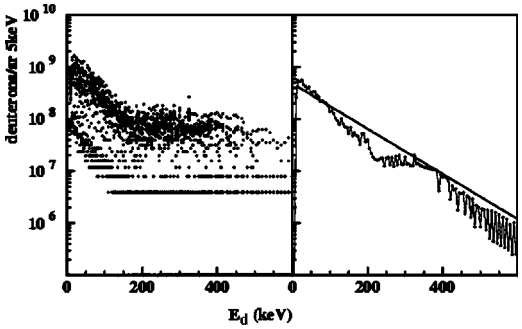

FIG. 3. Left panel: 21 randomly taken single-shot deuteron spectra during one experimental run. Right panel: average of the 21 spectra and compared with an exponential spectrum with a $kT_d = 100$ keV.

III. DEUTERON SPECTRA FROM SINGLE-DROPLET TARGETS

The ion emission has been previously measured with Thomson spectrometers from intense-laser-exposed heavy-water droplets [22,23] as to their energy and angular emission characteristics. The measured deuteron emission in absolute terms allows us to calculate the fusion-neutron signal when the energetic deuterons impinge on deuterized matter (secondary targets). With the calculated neutron yield from the deuteron irradiation geometry we calibrate the detection system. Furthermore, the quantitative measurement of ions emitted in different directions provides an important benchmark for a complex modeling of the laser-driven ion acceleration process.

The data of 21 single-shot deuteron spectra are depicted in the left panel of Fig. 3. They were taken in plane at 135° to the laser axis (Fig. 1) and were randomly selected during one run. The geometry of the Thomson spectrometer allowed us to record deuterons with energies E_d above 10 keV ($E_d \geqslant 10$ keV). The calculated mean of the 21 spectra is compared in the right panel of Fig. 3 with an exponential distribution:

$$d^2N_d/d\Omega\, dE = (1.2 \times 10^9/4\pi)\exp(-E_d/T_d)\ (\mathrm{sr}^{-1}\,\mathrm{KeV}^{-1}) \tag{1}$$

and a deuteron temperature parameter $T_d = 100$ keV. This corresponds to a total yield of 1.2×10^{11} deuterons into 4π sr

while the integrated mean spectrum amounts to 1.0×10^{11} deuterons into 4π sr. As will be shown below from the measured neutron intensity, with a secondary target of definite size an integral deuteron emission between 5×10^{11} and 8×10^{11} deuterons into 4π sr is deduced. This is also an important independent proof of the deuteron emission estimated from the spectrometer data. From these numbers it follows that about (0.2–0.3)% of all deuterons contained in the 20 μm droplet are accelerated to energies larger than about 10 keV. These energetic deuterons consume several percent of the incident laser energy. A similar temperature of 100 keV and a yield of 4.2×10^{11} deuterons has been reported [13] for a comparable target system using an 80 fs Ti:sapphire laser focused to a spot size of 3 μm and an intensity of 3×10^{19} W/cm^2.

For simulation calculations either the mean spectrum up to a maximum energy of 600 keV or the approximated spectrum is used in the following sections. For the calculation of the neutron spectra produced in secondary targets the above mean deuteron spectra were employed assuming isotropic emission from the surface of the target droplet. The neutron yield at the position of the neutron detectors was calculated by employing the $D(d,n)$ reaction angular differential cross section in the laboratory system [24,25] as a function of the relative angle between the incident deuteron and the neutron emitted in the direction of one of the neutron detectors as seen from the secondary target and the deuteron energy at the interaction point. The integration is performed over the solid angle subtended by the secondary target relative to the target droplet, the deuteron energy between 5 and 600 keV in the case of the mean deuteron spectrum, and the thickness of the secondary target. The energy loss of deuterons in polystrol $(CD)_n$ or heavy-water D_2O was calculated with the TRIM code [26]. In the case of the neighboring secondary droplet targets (SDTs) the different target thicknesses as a function of the irradiation angle is taken into account. The time of flight t is the sum of the deuteron TOF from the target droplet to the reaction point in the secondary target plus the neutron TOF from this position to the neutron detector. The calculated TOF spectra have been folded with an experimental TOF resolution of 3 ns full width at half maximum.

IV. SHOT-TO-SHOT CORRELATIONS

The amplitudes of the so-called plasma diode signals showed very large shot-to-shot variations. In the present case these fluctuations can be partly ascribed to the random probability of peripheral or central laser-droplet or no interaction at all. Furthermore variations in the laser beam intensity or time structure or even sideward deflections of either the droplet chain or the laser beam pointing can be the origin of shot-to-shot fluctuations. These fluctuations could not be controlled in the experiment. We performed a detailed statistical analysis of the correlations of observables characterizing the laser-target interactions from either shot to shot or different signals within one shot. The main results are summarized below.

Since the plasma diode was employed in the following to determine the neutron intensity per laser shot it was of special interest to investigate the correlation of target emission fluctuations in the optical range with the intensity of deuteron and γ emission. For this purpose the CCD camera was removed from the Thomson spectrometer and photodiodes were mounted in a frame such that they could detect a small part of the deuteron spectral trace visible on the phosphorus screen of the MCP. Thus the amplitude of the diode signal is proportional to the number of deuterons for an energy interval defined by the position of the diode on the screen and the size of the illuminated diode chip. These signals and those from the plasma light diode together with the prompt γ pulse have been registered with the data acquisition system.

We calculated the degree of the correlation between two different observables averaged over N_{shots}. The correlation between the deuteron emission in different energy intervals is about +0.8. From the similar correlation of about +0.7 between the deuteron emission signal and the plasma diode signal we can conclude that the measured plasma light amplitude correlates sufficiently with the deuteron emission signals. Therefore we used the plasma light diode signal for analysis of the neutron detection described in the next section and kept the CCD camera for observation of a few randomly selected deuteron emission spectra.

V. DEUTERON EMISSION FROM SINGLE DROPLETS AND NEUTRON DETECTION CALIBRATION

During the first experimental runs it became obvious that the neutron time-of-flight spectrum was subjected to signals which hardly could come from the original target source and the laser interaction point. The interior of the target chamber was changed in order to keep the influence of possible undefined sources of secondary neutron generation as low as possible.

In respect of the spherical symmetry of the target and the observed angular emission characteristic in our experiment [22] we refer here to inward and outward accelerated deuterons from the droplet. In order to infer data for the inward accelerated deuterons a careful analysis of the whole target system is indispensable. A closer look at the target system itself reveals that obviously the neighbor droplets in the train of droplets cannot be neglected. Thus we have two SDTs one above and one below the primary droplet target (Fig. 2) which are faced by the target droplet with a solid angle of about 2×90 msr for a distance between two droplets (center to center) of about 70 μm and a diameter of 20 μm (see scheme in Fig. 2). In the following we discuss the contribution of these droplets to the neutron signal on the basis of measurements with and without additional secondary targets.

The quantification of different neutron sources in the experiment requires a careful calibration of the whole detector arrangement at first. This also includes the control if deuteron and neutron emission signals can be registered consistently. Then we can resolve the contribution of the SDTs to the neutron signal and finally characteristics of the deuteron acceleration can be inferred, which is one major aim of this work. In order to investigate the uncertainties of the neutron detection efficiencies of all four detectors a secondary target was chosen in such way that the produced neutron time-of-

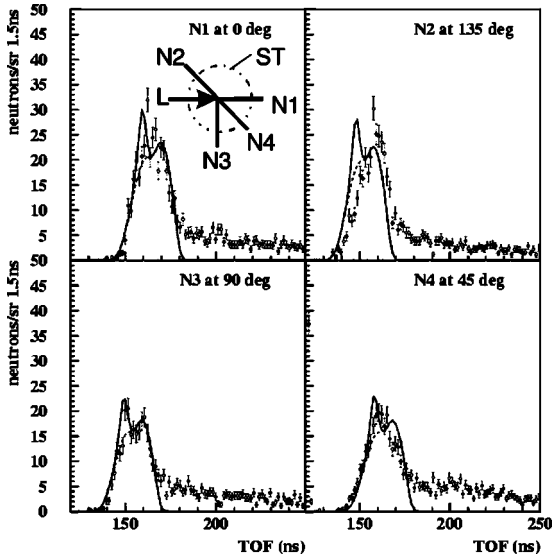

FIG. 4. Neutron spectra obtained with a secondary 2 mg/cm^2 thick deuterized polystrol target (ST) on Al-disk backing at 2.1 cm below the irradiated droplet. The path lengths of the neutron detectors N1–N4 were 347, 322, 325, and 344 cm, respectively. The solid line is the result of a calculation which was normalized by assuming $\sim 5\times 10^{11}$ deuterons into 4π sr; the scaling factor varied by about 35% for the different detectors. The inset shows the detection geometry.

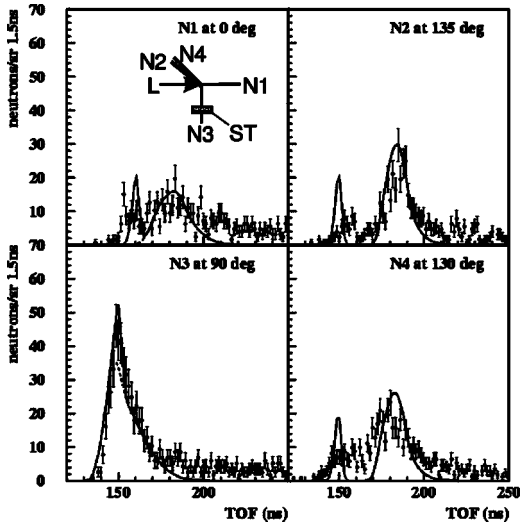

FIG. 5. Measured neutron spectra (open circles) obtained with a secondary deuterized polystrol target (ST) at 90° and 9.5 cm distance from the irradiated droplet along the line of sight of detector N3. The solid line is the result of simulation calculations employing the mean deuteron spectrum of Fig. 2 (right panel) assuming 8.3 $\times 10^{11}$ deuterons into 4π. The path length of the neutron detectors N1–N4 were 349, 326, 327, and 325 cm, respectively. The inset shows the detection geometry.

flight and intensity distributions are the same for all four neutron detectors. This was achieved by positioning concentric to the line of droplets and 2.1 cm below the laser focus a circular secondary target as described in Sec. II and Fig. 2. Since all detectors have similar distances to the secondary target the TOF distributions should be also similar. This expectation for the TOF spectra agrees well with the measured number of neutrons per sr, 1.5 ns, and laser shot as shown in Fig. 4. At 0°, 45°, 90°, and 135° the integrated neutron yield results in 377 ± 8, 288 ± 7, 277 ± 7, and 342 ± 8 neutrons per sr and laser shot, respectively. The integration was performed between 140 ns and 185 ns for N1 while for the other detectors slightly different path lengths were taken into account. The given errors for each detector are only statistical. The deviation between two detectors of up to 35% is far outside the statistical errors which we ascribe to a systematic uncertainty of the actual detection thresholds after a large γ flash.

Two effects cause the broad width of the peak in the TOF distributions shown in Fig. 4. The first is the large variation of the reaction angle (45°–135°) between the deuterons incident on the target disk and the emitted neutrons, which results in a considerable variation of the energy and the TOF of the neutrons due to the D(d,n) kinematics. Second, the variation of the TOF of the deuterons traveling over the 2.1–3.1 cm from the target droplet to the secondary target further broadens the TOF signal of the neutrons. The solid line in Fig. 4 shows the calculated neutron intensities [27] with the known thicknesses of the three secondary targets (two droplets and one disk) and an absolute outward emitted number of 5×10^{11} deuterons into 4π sr. This absolute number of deuterons has been obtained from the normalization of the calculation to the experimental data.

In order to deduce the number of neutrons produced in the PDT the neutrons produced in the SDTs have to be subtracted. This requires in principle a simultaneous measurement of the deuterons emitted into the direction of the SDTs for calculating the SDT neutron yield. Because this is not possible we assume in the following that (i) the deuteron spectrum is the same in and out of the plane which is defined by the incident laser beam axis and the laser polarization and (ii) the geometry of the droplet train as depicted in Fig. 2 is known. Additionally to the data from the Thomson spectrometer and in order to access on line all shots which produce energetic deuterons in one run we have chosen another secondary 9.5×9.5 cm^2 2 mg/cm^2 deuterated polystrol target. It was positioned in plane at 90° relative to the laser beam and 9.5 cm from the target droplet. This secondary target (cf. the "catcher" target in [13]) is employed as a monitor for the absolute normalization of the spectral intensity via the measured neutron yield which is measured with the four neutron detectors. Compared to the 0.007 cm distance to the SDTs the additional time of flight of the deuterons over 9.5 cm is much larger. This additional time let the neutrons from this secondary target appear in a TOF region well separated from the neutrons produced in the upper and lower droplets. This is not true, however, for those detectors which are in line with the deuteron flight path from the PDT to the secondary target plate, as for instance N3 (cf. the inset in Fig. 5). The thus obtained neutron time-of-flight spectra are shown in Fig. 5.

The spectra in Figs. 4 and 5 (and Fig. 7 below) manifest the experimental observation of a considerable background which is not understood. In order to investigate the background in more detail a 100 cm long polyethylene shadow bar was positioned between the neutron detector N2 and the

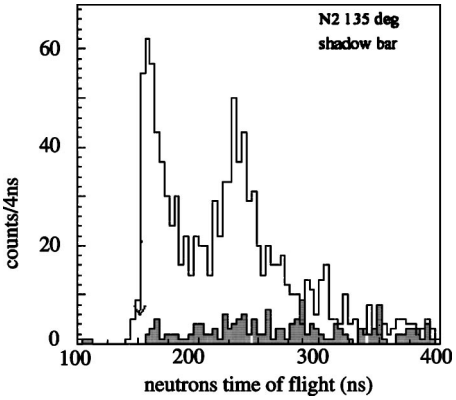

FIG. 6. Comparison of detected neutron signals when the source is shielded or not with a shadow bar: the residual signal due to scattering of the laboratory geometry is reproduced in calculations (cf. text).

target system. The shadow bar blocks all neutrons coming directly from the target region within a radius of about 10 cm–15 cm from the laser focus. The result of one run with and without the shadow bar is displayed in Fig. 6. The scattering of 2.5 MeV neutrons from structures in the MBI target room area was calculated with the code FLUKA [28]. The detailed calculations showed that we would expect only about 8% of the neutron signal between 140 and 175 ns in the TOF region between 180 and 250 ns. This is corroborated by the shadow bar measurement displayed in Fig. 6. But in the absence of the shadow bar (especially in Fig. 7 below) we observe an integral background between 130% and 170% concerning the neutron target signal. Clearly this background must come from other sources than in-scattered neutrons from the target. This assumption is corroborated by the finding that the background does not scale with the number of primary neutrons produced in secondary targets as can be seen in Fig. 4 where the peak to background ratio is considerably improved compared to Fig. 7 (see below). A possible reason for the enhanced background signal could be an additional deuteron interaction with D_2O contamination layers inside the chamber.

VI. NEUTRON SPECTRA FROM A DROPLET TARGET SYSTEM

Because the following analysis will show that it is hard to distinguish between different contributions of the neutron emission we start the discussion with neutron generation from the neighbor droplets (SDTs). The obtained signal distribution in Fig. 4 can be already reasonably well reproduced without a neutron contribution from the PDT by simulation calculations. The slightly enhanced first peak comes from the superimposed neutron signal from the two SDT droplets. Although the irradiation solid angle of the disk is about ten times larger than that of both SDTs the neutron signal from the SDTs is nicely visible in the simulation and in the data. The dashed line in Fig. 4 shows only the contribution from the disk target (ST) which produces an almost double humped distribution. This shape is due to the above mentioned variation of the neutron energy for forward and backward emitted neutrons relative to the deuteron trajectory.

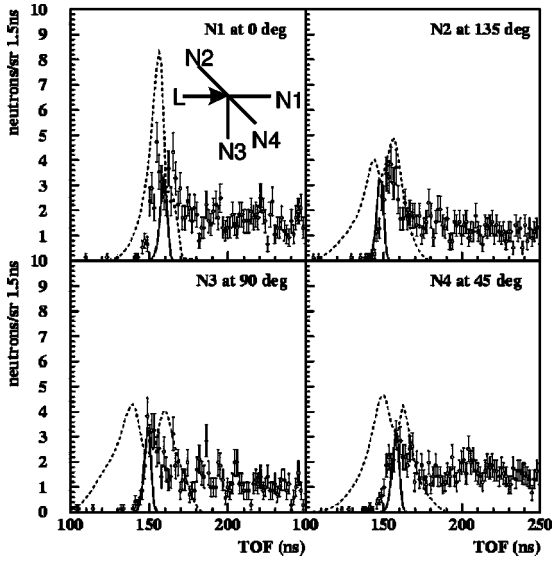

FIG. 7. Neutron spectra without an additional secondary target. The solid line is the result of simulation calculations and corresponds to neutrons produced in the SDTs assuming 8.4×10^{10} deuterons into 4π sr and a temperature of 100 keV. The dashed line is the result of simulation calculations employing the PIC model calculations for the energy and angular distributions of deuterons published in Ref. [5] with a total yield of 5×10^9 deuterons. The path lengths of the neutron detectors N1–4 were 347, 322, 325, and 344 cm, respectively. The inset shows the detection geometry.

The broad peaks in Fig. 5 around 180 ns in the TOF spectra of detectors N1, N2, and N4 are due to neutrons produced in the secondary deuterated polystrol target while the small peak at about 150 ns–160 ns is due to neutrons produced in the SDTs. In the case of detector N3 the two contributions are superimposed. From the normalization of the model calculations to the measured broad peaks of N1, N2, and N4 a deuteron emission of 8.3×10^{11} into 4π sr per pulse was deduced. The dashed line in the N3 spectrum represents only the contribution from the polystrol target while the solid line corresponds to the sum of all three secondary targets. The measured TOF spectra are reasonably well described by the calculations, except that the narrow peak structure of the droplet contributions is not reproduced by the measurements.

The calculated spectrum differs considerably from the experimental one in the vicinity of the DT peak (at 140 ns to 160 ns) for the detectors N1, N2, and N4. The fraction of experimentally observed and calculated neutron yield within the base width of the narrow SDT peak is found to be 40%–80%. Consequently only the complement can be due to reactions within the actual target droplet hit by the laser beam. In comparison one can calculate from the experimental data published in [13] a lower SDT contribution of about 20%. In summary, for our droplet-train target system and for the irradiation conditions used we can conclude that a large fraction of the measured neutron yield with neutron energies between 2 MeV and 3 MeV is due to neutron production in the heavy-water droplets neighboring the laser-irradiated droplet. This implies a low neutron yield because

the majority of the energetic deuterons do not contribute to the neutron signal.

Finally we discuss in the following the experimental results when no additional secondary target was placed inside the target chamber except for the always present SDTs. The neutron TOF distributions for the four detectors are displayed in Fig. 7. The experimental data are compared with two calculations. The first one, indicated by the solid line, stands for the neutron signal from the SDTs irradiated with a total of 8.4×10^{10} deuteron per shot with a temperature of 100 keV. Since the $D(d,n)$ reaction angles are close to 90° for the SDT neutrons their energy is close to 2.45 MeV. Compared to the calculated TOF distributions the measured distributions are much broader at all angles and show an extended tail to longer TOFs. We consider at least a part of this tail above 180 ns as background.

Second, the data are compared with a calculated neutron signal which would arise from a simulated deuteron dynamics inside the droplet. Especially we want to proof how sensitively the neutron spectra depend on a specific deuteron acceleration [13]. We assumed in the calculation that these deuterons are originating in the center of the target droplet and experience an effective target thickness of 1.1 mg/cm^2 D_2O.This is one main endeavor of our work: that we can use the data taken with the complex neutron-detection setup in order to infer the deuteron dynamics inside the dense target. The angular and energy distributions of the deuterons have been taken from the particle-in-cell (PIC) calculation published in [13] by fitting the spectra in seven angular ranges by a two-temperature exponential function. Our comparison is only of qualitative character, because the laser parameters in [13] and also the focusing conditions are not identical to ours (see above). The total yield was reduced to 5×10^9 deuterons compared to 1.0×10^{11} employed in [13]. The result of the simulation is shown by the dashed line in Fig. 7. The shape of the simulated curve, i.e., the double humped distribution for detectors N1, N2, and N4 results from the fact that the deuteron angular and energy distributions are peaked perpendicular to the laser-beam axis (Fig. 3 of Ref. [13]). Our experimental data, however, differ clearly from this calculation at 135°, 45°, and particularly at 90°. At 0° the calculated distribution is somewhat similar to the experimental data. This is due to the fact that at this angle the neutrons are viewed essentially at 90° to the deuteron direction and consequently due to kinematics the neutron energy is not very sensitive to the deuteron energy. The largest sensitivity for a comparison with such a model for the deuteron acceleration in a droplet is clearly the neutron TOF or energy distribution at 90° to the laser beam. The obvious disagreement between simulation and experiment at this angle as well as at the other three angles shows that under our conditions a spatially peaked distribution of accelerated deuterons perpendicular to the laser axis is obviously not apparent inside the droplet.

VII. SHIFTS IN NEUTRON ENERGY SPECTRA

A more detailed comparison of the experimental data with the calculation for the SDTs (solid line in Fig. 7) as a reference for 2.45 MeV neutrons reveals that the TOF seems to

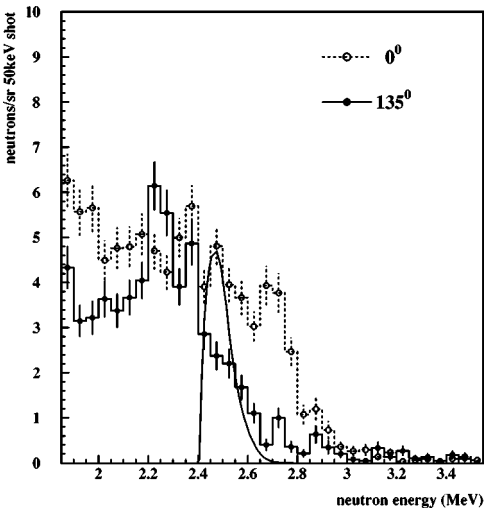

FIG. 8. Neutron energy spectra at 0° and 135° (sum of runs 334, 337, 338, 411, 413, and 435). The neutron yield integrated between 2 MeV and 3 MeV amounts to 72 and 48 n/sr shot at 0° and 135°, respectively. The thin curve at about 2.45 MeV corresponds to the expected neutron energies from reactions in the neighbor droplets.

be shifted at 0° and 45° to lower and at 135° to higher TOFs corresponding to higher and lower neutron energies compared to 2.45 MeV. A similar observation was made in all runs. In order to investigate this finding further we transformed the TOF into energy spectra at two angles. This can be done for those neutrons which are produced very close to the target droplet and inside the irradiated droplet. In Fig. 8 we show the summed energy spectra for a forward (0°) and a backward detector (135°). In order to get reasonably good statistics we summed up six runs with a total number of 3.5×10^5 laser shots or 9 h of laser running time. The neutron energies below 2 MeV cannot be taken into account because also runs have been used where corresponding neutron TOFs are increased by deuteron exposure of a separated secondary target. The energies above about 2 MeV should be correct. Neutrons in the forward direction (0°) are more energetic than those in the backward direction (135°) which indicates that these neutrons must have been produced inside the target droplet by energetic deuterons preferentially moving in the forward direction. This finding is corroborated by the observation that the energy deviations are almost symmetric to 2.45 MeV: about +300 keV at 0° and −200 keV at 0°. This is very similar to the reported [8] neutron energy distributions in a solid target. This means that those deuterons which are accelerated inside the dense droplet are mainly moving along the incident laser axis. In contrast to the radially accelerated deuterons from the droplet surface outward, the inward accelerated deuterons do not feel the target geometry. The thin solid curve represents the expectation for the SDTs as calculated with the deuteron spectrum from Fig. 3. Especially for this analysis it is important to note that the signal from the SDTs is much less broadened than the measured energetic shifts. The observed shoulder at 2.5 MeV of the energy distribution at 135° and the broad structure at 0° can be interpreted as the contribution from the SDTs as already discussed above. The yield around 2.25 MeV for the

0° detector is, however, inconsistent with the picture of neutrons produced inside the target by forward moving energetic deuterons only. The yield in this region should show a minimum in order to be consistent with the 135° distribution. One could assume that the origin of this residual signal is due to unresolved secondary neutron emission as discussed in Sec. V.

The integrated yield between 2 and 3 MeV amounts to 70 and 40 n/sr shot in the forward and backward directions, respectively, which corresponds to a total neutron production of about 700 n/shot. The finding of a two times larger yield in the forward direction should be considered with some caution due to the uncertainty in the efficiencies as well as possible background contributions. It should be mentioned that the neutron yield was found to be up to a factor of 3 larger if only laser shots are selected that produced a large signal in the plasma diode.

In summary, under our experimental conditions the irradiated droplet contributes only marginally to the measured neutron signal while a considerable fraction is due to neutron production in the SDTs. Those neutrons from the PDT emitted in the forward direction are more energetic than backward emitted neutrons, which is similar to the observations with a solid target [8]. Thus we find indications that deuterons inside the droplet are accelerated preferentially along the incident laser propagation. This coincides with simulations for plane solid targets [7].

VIII. NEUTRON SPECTRA FROM A HEAVY-WATER SPRAY TARGET

Because droplets of 20 μm extension are already an efficient ion emitter when they are exposed to an intense laser pulse we developed a different spray source [17]. The main idea for this target concept is similar to the use of cluster ensembles. A number of objects that are smaller than the laser wavelength are exposed to a certain laser intensity which leads to efficient laser energy absorption and explosion of the tiny objects. Ions from the exposed objects acquire considerable energy during that process and collide with each other and the surrounding cold matter in the spray. The advantage of the spray source compared to pure D clusters [10] or CD_4 clusters [11] relies on the larger extension (150 nm in diameter) of the heavy-water microspheres. If such objects are exposed to very high laser intensities a similar interaction scenario as in the case of the bigger microdroplet takes place: a high electric field strength is built up around the microdroplets due to charging and formation of a double electric layer—the acceleration sheath. This in turn leads to outward directed deuteron acceleration and kinetic energies of several 100 keV up to 1 MeV (similar results for protons are given in [18]) are achieved which are significantly higher compared to cluster explosions [12]. The corresponding increase of the cross sections of the fusion reaction allows us to anticipate a higher efficiency for the fusion neutron output in relation to the deuteron number or the laser-irradiated volume from which they are produced.

The laser beam was focused up to $\sim 10^{19}$ W/cm^2 with the same optic as in the droplet experiment. The position of the focus was close below the nozzle within the 2 mm extended cloud of 10^{11} cm^{-3} microspheres. The measured neutron signals have a lower statistics because the spray injection rate had to be reduced to 12 s while the laser was running at 10 Hz. Still the γ flash was at a level which hinders moving the scintillator detectors closer to the chamber for the sake of a higher counting rate. The spectrometer setup was slightly changed during the spray experiments. In addition to the Thomson parabola spectrometer (cf. Fig. 1) only two neutron detectors (N1,N2) were positioned at observation angles of 0° (laser propagation) and 135°.

The neutron emission has been calculated with the deuteron emission spectrum and assuming for a simple model calculation a sphere of cold D_2O matter around the interaction point. The angular distribution of the emitted deuterons is assumed to be isotropic. The sphere radius is 1 mm and the effective areal density of 18 μg/cm^2, as seen from the center of the cloud, is deduced from the average density within the 2 mm extended cloud. Due to the interaction geometry all D(d,n) reaction angles between 0° and 180° are possible, resulting in high and low energies for forward and backward emitted neutrons. Using 8×10^{10} deuteron emission into 4π sr the calculation reproduces quite well the experimental data. From all the shots a value of 500 ± 60 and 515 ± 60 neutrons/sr and per pulse is obtained for two neutron detectors positioned at 0° and 135°, respectively, which amounts to a 3–10 times higher yield compared to the droplet target system. In our experiment the ions have favorably higher energies compared to previous cluster experiments [10–12] which is the most striking difference. Thus the lower average density and smaller laser-target interaction volume as realized in cluster experiments can be compensated. Therefore we can achieve a similar neutron emission as recently published from cluster sources [12]. This neutron number is efficiently produced from a much smaller laser-irradiated volume compared to previous cluster experiments. That offers an interesting scaling option concerning the neutron number. A more quantitative comparison to cluster sources will be discussed in a forthcoming paper [29] and the trade-off between a longer interaction channel and a related lower laser interaction intensity has to be studied in future experiments.

IX. CONCLUSIONS

Inward and outward laser-driven acceleration of deuterons was studied from microdroplets by means of high resolution neutron spectroscopy of the initiated D(d,n) reaction. In addition to the investigation of the acceleration kinetics of the deuterons the related emission of neutrons has been determined in absolute terms.

Our interaction experiments with laser pulses of $\sim$40 fs width and up to 10^{19} W/cm^2 intensity have shown that microdroplets of 20 μm extension can emit efficiently ions in the energy range between 10 keV and several MeV. As a result of the mainly outward directed acceleration the number of fusion collisions inside the droplet is limited, which results in a neutron yield of 700–1400 n/shot. This should be compared with $(6-9)\times10^4$ neutrons per shot which one

might expect if all $5-8\times10^{11}$ deuterons emitted from the droplet surface were stopped in a spherical shell of 2 mg/cm^2 heavy water around the droplet target. In order to approach such a situation one could enlarge the target dimension, which would lead in consequence to a plane solid target. Here we realized a different solution for exploiting the deuteron emission characteristic of microspheres. A spray target which represents an ensemble of microspheres of 150 nm extension has been shown to deliver 6000 neutrons per pulse. The striking feature of this target system turned out to be the generation of deuterons with kinetic energies up to the MeV range. This results in efficient fusion neutron production from a much smaller laser-irradiated volume as compared to recently published cluster experiments. But still, with all the attempts made in this and in other work with cluster sources, the neutron flux from a directly laser-exposed solid deuterated target could not be overtaken. Such a solid target resembles a deuteron source and an adjacent secondary target which seems to work most efficiently for tabletop laser-driven neutron sources. In order to envision experiments where, e.g., a neutron pulse induces damage in a material, necessary neutron fluxes of $\geqslant10^9\ n/cm^2\,s$ have been estimated [30]. Starting from the present experimental data an increase of several orders in the neutron yield has to be pursued in order to meet this requirement.

The applied neutron diagnostics is a powerful method. The presence of a very intense prompt electron and γ pulse preceding the neutron pulse prevents us, however, from exploiting fully the possibilities of this method. Nevertheless, we could determine that in our experiments deuteron acceleration into the droplet causes only a small part of the neutron yield while a considerable fraction is due to $D(d,n)$ reactions in the neighboring droplets. The neutrons produced in the forward direction (0° and 45°) are found to be more energetic than neutrons emitted in the backward direction (135°). Our result is similar to the findings obtained with a solid plane target. A deuteron acceleration along the laser axis in the dense target is inferred. The obtained data provide benchmarks for further modeling.

ACKNOWLEDGMENTS

The authors thank H. Schönnagel and E. Risse for providing substantial work in realization of the relevant Ti:sapphire HFL parameters and L. Pienkowski from the University of Warsaw for performing the FLUKA calculations. The work was partly supported by DFG Project SFB-Transregio TR18.

[1] M. Hegelich, S. Karsch, G. Pretzler, D. Habs, K. Witte, W. Guenther, M. Allen, A. Blasevic, J. Fuchs, J.C. Gauthier, M. Geissel, P. Audebert, T. Cowan, and M. Roth, Phys. Rev. Lett. **89**, 085002 (2002).

[2] M. Zepf, E.L. Clark, F.N. Beg, R.J. Clarke, A.E. Dangor, A. Gopal, K. Krushelnick, P.A. Norreys, M. Tatarakis, U. Wagner, and M.S. Wei, Phys. Rev. Lett. **90**, 064801 (2003).

[3] S.P. Hatchett, C.G. Brown, T.E. Cowan, E.A. Henry, J.S. Johnson, M.H. Key, J.A. Koch, A.B. Langdon, B.F. Lasinski, R.W. Lee, A.J. Mackinnon, D.M. Pennington, M.D. Perry, T.W. Phillips, M. Roth, T.C. Sangster, M.S. Singh, R.A. Snavely, M.A. Stoyer, S.C. Wilks, and K. Yasuike, Phys. Plasmas **7**, 2076 (2000).

[4] M. Borghesi, S. Bulanov, D.H. Campbell, R.J. Clarke, T.Zh. Esirkepov, M. Galimberti, L.A. Gizzi, A.J. MacKinnon, N.M. Naumova, F. Pegoraro, H. Ruhl, A. Schiavi, and O. Willi, Phys. Rev. Lett. **88**, 135002 (2002).

[5] M.I. K. Santala, M. Zepf, F.N. Beg, E.L. Clark, A.E. Dangor, K. Krushelnick, M. Tatarakis, I. Watts, K.W. D. Ledingham, T. McCanny, I. Spencer, A.C. Machacek, R. Allott, R.J. Clarke, and P.A. Norreys, Appl. Phys. Lett. **78**, 19 (2001).

[6] M. Yamagiwa and J. Koga, J. Phys. D **32**, 2526 (1999).

[7] H. Habara, R. Kodama, Y. Sentoku, N. Izumi, Y. Kitagawa, K.A. Tanaka, K. Mima, and T. Yamanaka, Phys. Plasmas **10**, 3712 (2003).

[8] D. Hilscher, O. Berndt, M. Enke, U. Jahnke, P.V. Nickles, H. Ruhl, and W. Sandner, Phys. Rev. E **64**, 016414 (2001).

[9] G. Pretzler, A. Saemann, A. Pukhov, D. Rudolph, T. Schätz, U. Schramm, P. Thirolf, D. Habs, K. Eidmann, G.D. Tsakiris, J. Meyer-ter-Vehn, and K.J. Witte, Phys. Rev. E **58**, 1165 (1998).

[10] T. Ditmire, Nature (London) **398**, 489 (1999).

[11] G. Grillon, Ph. Balcou, J.-P. Chambaret, D. Hulin, J. Martino, S. Moustaizis, L. Notabaert, M. Pittman, Th. Pussieux, A. Rousse, J.-Ph. Rousseau, S. Sebban, O. Sublemontier, and M. Schmidt, Phys. Rev. Lett. **89**, 065005 (2002).

[12] K.W. Madison, P.K. Patel, D. Price, A. Edens, M. Allen, T.E. Cowan, J. Zweiback, and T. Ditmire, Phys. Plasmas **11**, 270 (2004).

[13] S. Karsch, S. Düsterer, H. Schwoerer, F. Ewald, D. Habs, M. Hegelich, G. Pretzler, A. Pukhov, K. Witte, and R. Sauerbrey, Phys. Rev. Lett. **91**, 015001 (2003).

[14] K.W. Madison, P.K. Patel, M. Allen, D. Price, and T. Ditmire, J. Opt. Soc. Am. B **20**, 113 (2003).

[15] L. Disdier, J.-P. Garconnet, G. Malka, and J.-L. Miquel, Phys. Rev. Lett. **82**, 1454 (1999).

[16] T. Ditmire, T. Donnelly, A.M. Rubenchik, R.W. Falcone, and M.D. Perry, Phys. Rev. A **53**, 3379 (1996).

[17] S. Ter-Avetisyan, M. Schnürer, H. Stiel, and P.V. Nickles, J. Phys. D **36**, 2421 (2003).

[18] M. Schnürer, S. Ter-Avetisyan, S. Busch, M.P. Kalachnikov, E. Risse, W. Sandner, and P.V. Nickles, Appl. Phys. B: Lasers Opt. **78**, 895 (2004).

[19] M.P. Kalachnikov, V. Karpov, and H. Schönnagel, Laser Phys. **12**, 368 (2002).

[20] Hemberg, B.A.M. Hansson, M. Berglund, and H.M. Hertz, J. Appl. Phys. **88**, 5421 (2000).

[21] S. Düsterer, Ph.D. thesis, FSU, Jena, 2003.

[22] S. Busch, S. Ter-Avetisyan, M. Schnürer, M. Kalashnikov, H. Schönnagel, H. Stiel, P.V. Nickles, and W. Sandner, Appl. Phys. Lett. **82**, 3354 (2003).

[23] S. Ter-Avetisyan, M. Schnürer, S. Busch, E. Risse, P.V. Nickles, and W. Sandner, Phys. Rev. Lett. (to be published).

[24] H. Liskien and A. Paulsen, Nucl. Data Tables **11**, 569 (1973).
[25] A. Boughrara, H. Beaumevieille, and S. Ouichaoui, Europhys. Lett. **48**, 264 (1999).
[26] J.P. Biersack and L.G. Haggmark, Nucl. Instrum. Methods **174**, 257 (1980).
[27] Fusion neutron computation using energy and collision angle dependent cross sections and deuteron propagation [D. Hilscher (unpublished)].
[28] Computer FLUKA, code version Oct. 2002, www.fluka.org
[29] S. Ter-Avetisyan, M. Schnürer, S. Busch, P.V. Nickles, and W. Sandner, Phys. Plasmas (to be published).
[30] J. Zweiback, T.E. Cowan, R.A. Smith, J.H. Hartley, R. Howell, C.A. Steinke, G. Hays, K.B. Wharton, J.K. Crane, and T. Ditmire, Phys. Rev. Lett. **85**, 3640 (2000).